Research Square

Preprints are preliminary reports that have not undergone peer review.
They should not be considered conclusive, used to inform clinical practice,
or referenced by the media as validated information.

Groundwater potential mapping of the Imiter region, Anti-Atlas, Morocco

El Mahdi BEN SAYAH

bensayah.m@gmail.com

Chouaib Doukkali University

Abdelmajid RAHIMI

Chouaib Doukkali University

Mariame KHOLAIQ

Chouaib Doukkali University

Research Article

Keywords: Groundwater potential, MCDA, weighted overlay, lineament density, hydrothermal alteration, ASTER, Sentinel-2, U/Th, Th/K, Anti-Atlas, Morocco

Posted Date: August 10th, 2026

DOI: https://doi.org/10.21203/rs.3.rs-10581684/v1

License: This work is licensed under a Creative Commons Attribution 4.0 International License.
Read Full License

Additional Declarations: No competing interests reported.

Groundwater potential mapping of the Imiter region, Anti-Atlas, Morocco

El Mahdi BEN SAYAH[1*], Abdelmajid RAHIMI[1] and Mariame KHOLAIQ[1]

[1*]Department of Geology, Faculty of Sciences, Chouaib Doukkali University, El Jadida, Morocco.

*Corresponding author(s). E-mail(s): bensayah.m@gmail.com

Abstract

Groundwater is a critical resource in the arid Imiter region of the central Anti-Atlas, Morocco, where surface water is scarce, and groundwater occurrence is mainly controlled by fracture-related secondary permeability, terrain conditions, and hydrothermal alteration. This study delineates groundwater potential zones (GWPZs) by integrating multisource remote sensing, morphostructural analysis, terrain-derived indices, and airborne radiometric data within a GIS-based multi-criteria decision analysis (MCDA) framework. Eight thematic factors were considered: lineament density, topographic wetness index (TWI), slope, drainage density, normalized difference vegetation index (NDVI), and three ASTER-derived hydrothermal alteration indicators, namely carbonate, kaolinite, and Fe^3 alteration. Slope, TWI, and drainage density were derived from SRTM-based terrain analysis, NDVI was calculated from Sentinel-2 imagery, lineament density was extracted from morphostructural analysis, and hydrothermal alteration layers were obtained from ASTER VNIR–SWIR data. The reclassified thematic layers were integrated using weighted overlay analysis, with lineament density assigned the strongest influence, followed by TWI, slope, drainage density, carbonate alteration, kaolinite alteration, NDVI, and Fe^3 alteration. The resulting GWPZ map reveals strong structural and morphometric controls on groundwater favorability, with high-potential zones preferentially concentrated along fractured corridors and hydrothermally altered domains, where terrain conditions favor infiltration and subsurface accumulation. To evaluate the model independently, single-band airborne radiometric layers of uranium, thorium, and potassium were used to calculate U/Th and Th/K ratios, which were then compared with the predicted GWPZ classes through point-based validation. A total of 5307 validation points were used. The Th/K ratio provided the strongest agreement with the groundwater-favorable zones, with an accuracy of 0.601, precision of 0.632, recall of 0.857, and F1-score of 0.728. The

U/Th ratio provided complementary support, with an accuracy of 0.537, precision of 0.571, recall of 0.828, and F1-score of 0.676. These results indicate that the proposed workflow provides a reproducible and physically meaningful framework for regional-scale groundwater prospectivity mapping in structurally complex arid hard-rock terrains.

Keywords: Groundwater potential; MCDA; weighted overlay; lineament density; hydrothermal alteration; ASTER; Sentinel-2; U/Th; Th/K; Anti-Atlas; Morocco.

1 Introduction

Groundwater represents one of the most strategic water resources in arid and semiarid regions, where surface water availability is limited, rainfall is irregular, and recharge processes are strongly constrained by climatic and geomorphological conditions (Scanlon et al. 2006; Taylor et al. 2013). In southern Morocco, these constraints are particularly pronounced, as recurrent drought, increasing agricultural demand, and the scarcity of perennial surface-water systems have intensified the need for reliable groundwater exploration tools (Echogdali et al. 2022; Ikirri et al. 2023; El Ayady et al. 2023). In such contexts, identifying groundwater-favorable zones is essential for improving water-resource planning, reducing uncertainty in field investigations, and guiding future hydrogeological and geophysical surveys (Kamaraj et al. 2023; Seqqam et al. 2025).

In hard-rock terrains, groundwater occurrence is rarely controlled by primary porosity alone. Instead, it is primarily governed by secondary permeability associated with fractures, faults, weathered zones, and structurally controlled pathways (Lachassagne et al. 2021). The effectiveness of these pathways is further influenced by topographic conditions, drainage organization, surface moisture indicators, and lithological or mineralogical transformations associated with fluid-rock interaction (Kamaraj et al. 2023; Subramani et al. 2024). This is particularly relevant in the Anti-Atlas of Morocco, where groundwater systems are generally discontinuous and spatially heterogeneous (Echogdali et al. 2022; Ikirri et al. 2023). In such settings, fractured corridors, altered zones, low-slope sectors, drainage convergence areas, and zones with favorable wetness conditions may collectively enhance infiltration, storage, and subsurface circulation (Lachassagne et al. 2021; El Ayady et al. 2023).

Remote sensing and geographic information systems provide an efficient framework for regional-scale groundwater prospectivity assessment, especially in areas where direct hydrogeological measurements remain sparse (Malczewski 2006; Echogdali et al. 2022; Ikirri et al. 2023). Satellite imagery, digital elevation models, and morphostructural analysis enable the extraction of thematic layers describing terrain morphology, vegetation cover, drainage organization, structural density, and alteration patterns (Drusch et al. 2012; Farr et al. 2007; Abrams and Yamaguchi 2019). These layers can then be integrated using multi-criteria decision analysis to produce groundwater potential zone maps (Malczewski 2006; Kamaraj et al. 2023; Seqqam et al. 2025). However, the reliability of such approaches depends strongly on the quality of the selected factors, the transparency of their reclassification, the logic of their weighting, and the use of independent validation data (Echogdali et al. 2022; Ikirri et al. 2023; El Ayady et al. 2023).

Many groundwater potential studies rely on weighted overlay or AHP–MCDA approaches because they offer a practical way to combine heterogeneous spatial variables (Malczewski 2006; Echogdali et al. 2022; Kamaraj et al. 2023). Nevertheless, several limitations remain common. First, the selection and weighting of factors may introduce subjectivity if not clearly justified. Second, thematic layers are often integrated without sufficient explanation of their hydrological meaning, especially when indirect proxies are used. Third, validation is sometimes limited to internal model consistency or to sparse field observations, which do not always demonstrate whether the predicted favorable zones are physically meaningful (Ikirri et al. 2023; El Ayady et al. 2023; Seqqam et al. 2025). These limitations are particularly important in fractured arid terrains, where groundwater occurrence is discontinuous and where conventional validation datasets, such as well-yield records or piezometric measurements, are often limited or unavailable (Lachassagne et al. 2021; Kamaraj et al. 2023).

The Imiter region, located in the central Anti-Atlas of Morocco, provides a suitable case study for addressing these issues. The area is characterized by arid climatic conditions, rugged topography, a dense fault network, and widespread hydrothermal alteration inherited from complex tectono-magmatic and hydrothermal processes (Cheilletz et al. 2002; Tuduri et al. 2006; Atif et al. 2022). Previous work in the region has demonstrated the usefulness of ASTER data for mapping hydrothermal alteration minerals, particularly carbonate, kaolinite, and Fe^{3+} alteration (Ben Sayah et al. 2023). These alteration patterns are not direct indicators of groundwater occurrence, but they may highlight zones affected by past fluid circulation, rock transformation, and structural weakening (Shebl et al. 2023; Gobashy et al. 2024). When combined with morphometric

and structural indicators, they provide useful indirect information for regional groundwater targeting (El Ayady et al. 2023; Kamaraj et al. 2023).

In this study, groundwater potential zones in the Imiter region are delineated using a GIS-based weighted-overlay MCDA approach that integrates eight thematic factors: lineament density, topographic wetness index (TWI), slope, drainage density, normalized difference vegetation index (NDVI), carbonate alteration, kaolinite alteration, and Fe^{3+} alteration. These factors were selected to represent the main controls on groundwater favorability in the study area, including secondary permeability, infiltration potential, drainage concentration, surface moisture conditions, and hydrothermal alteration related to fluid-rock interaction (Beven and Kirkby 1979; Tucker 1979; Abrams and Yamaguchi 2019; Lachassagne et al. 2021). Unlike approaches based only on internal weighting, the resulting groundwater potential map is further evaluated using independent airborne radiometric indicators derived from U/Th and Th/K ratios (Maden and Akaryali 2015; Shebl et al. 2023; Gobashy et al. 2024).

Accordingly, the objectives of this study are to: (i) derive and standardize the main morphostructural, topographic, vegetation, drainage, and hydrothermal alteration layers controlling groundwater favorability in the Imiter region; (ii) integrate these layers through a weighted-overlay MCDA framework to produce a groundwater potential zone map; and (iii) assess the spatial consistency of the predicted favorable zones using independent radiometric validation based on U/Th and Th/K ratios. By combining remote sensing, terrain analysis, structural interpretation, hydrothermal alteration mapping, and geophysical validation, this study aims to provide a reproducible workflow for groundwater prospectivity assessment in structurally complex arid hard-rock terrains.

2 Study Area

The study area is located in the central Anti-Atlas Mountains of southeastern Morocco, between latitudes 30°20′N and 31°00′N and longitudes 5°50′W and 6°30′W. It corresponds to the Imiter region, which forms part of the Saghro inlier within the Ouarzazate–Tinghir structural domain (Walsh et al. 2012; Cheilletz et al. 2002; Tuduri et al. 2006). The area is characterized by rugged topography, pronounced elevation contrasts, and deeply incised valleys, which exert important control over runoff, infiltration, and groundwater recharge (El Qorchi et al. 2023). As shown in Fig. 1, the

study area is situated within the central Anti-Atlas, highlighting its position in a structurally complex and arid environment.

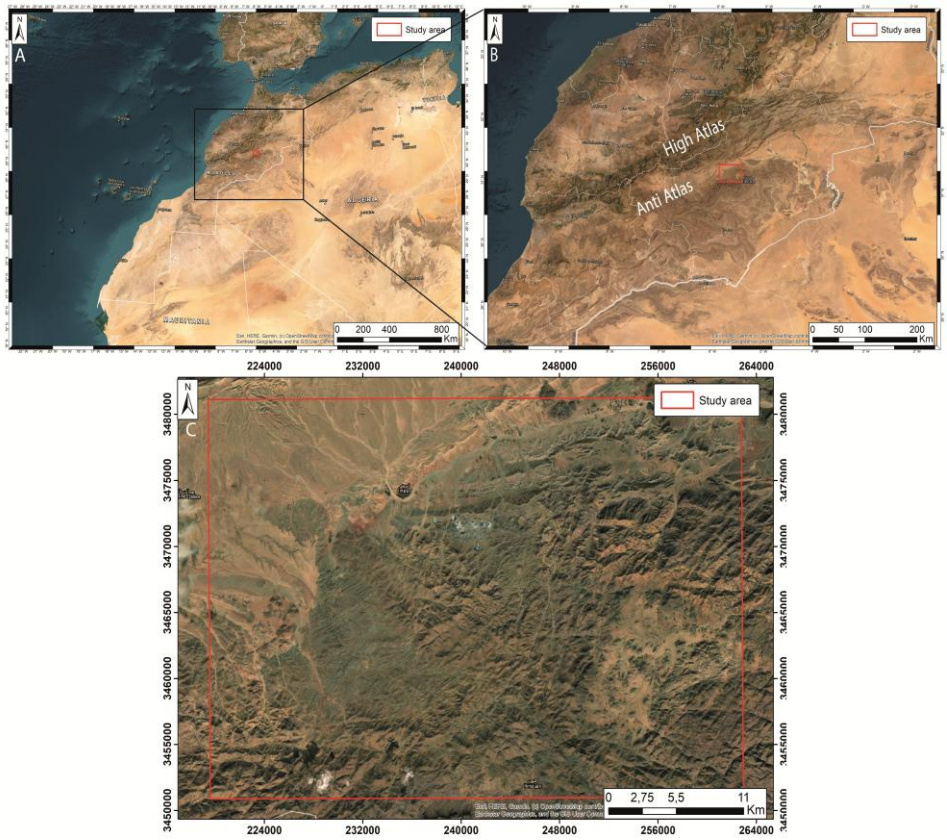


Fig. 1 Location maps of the study area: (A) North Africa, (B) Morocco, and (C) Imiter study area (Anti-Atlas, southeastern Morocco).

Geologically, the Anti-Atlas constitutes the northern margin of the West African Craton and is composed of a Neoproterozoic basement overlain by Paleozoic sedimentary successions later affected by Hercynian deformation (Soulaimani et al. 2018; Walsh et al. 2012). Within the Imiter inlier, the exposed lithologies include quartzites, shales, volcaniclastics, dolerites, and carbonate formations, which are locally affected by hydrothermal alteration associated with Precambrian and Variscan tectonic events (Cheilletz et al. 2002; Tuduri et al. 2006; Atif et al. 2022). Major structural lineaments, including the Imiter, Bou Azzer, and Saghro fault systems, play a key role in organizing the area's geological framework. In hydrogeological terms, these major fault corridors are of particular importance because they enhance secondary permeability and act as preferential pathways for groundwater circulation, while also controlling the

localization of hydrothermal fluid flow and ore deposition (Cheilletz et al. 2002; Tuduri et al. 2006; Atif et al. 2022). As illustrated in Fig. 2, the geological framework of the Imiter area highlights the spatial distribution of the main lithological units and major structural discontinuities controlling groundwater occurrence.

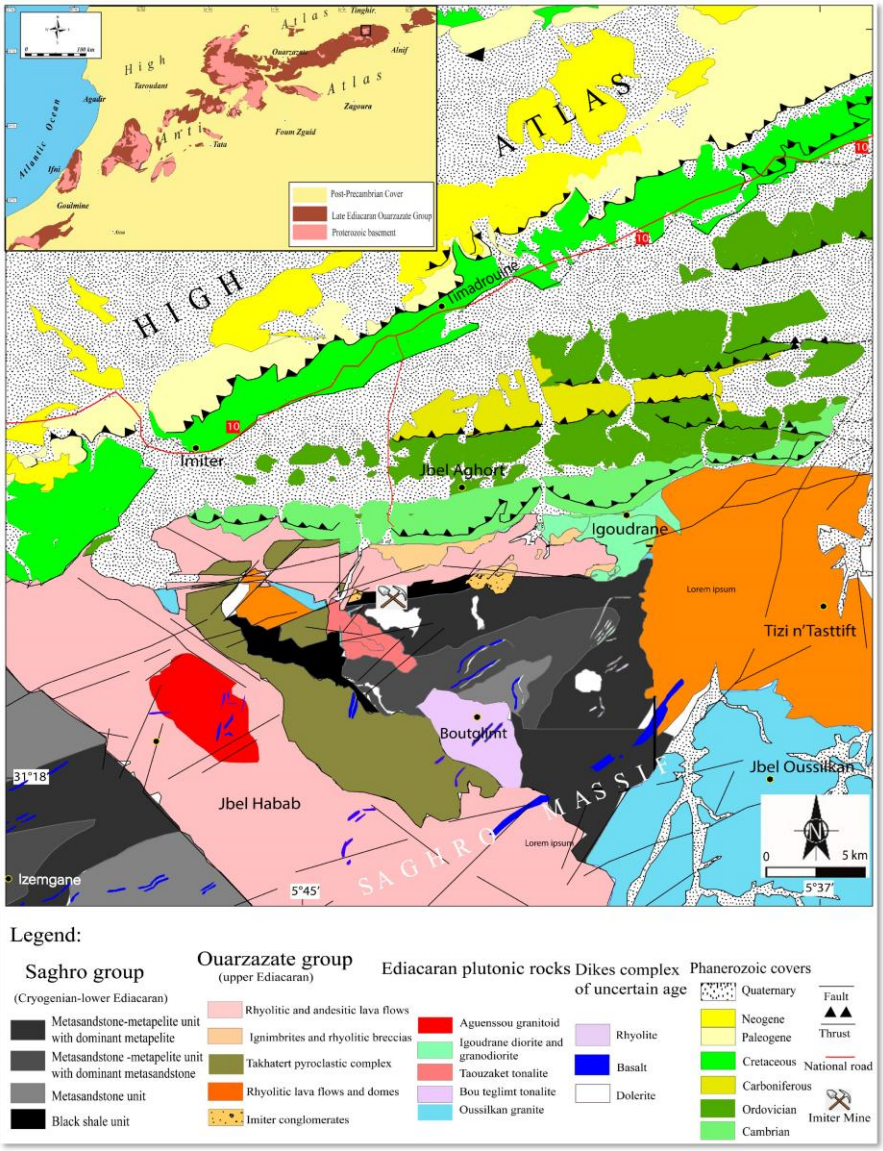


Fig. 2 Geological map of the Imiter study area

Hydrogeologically, the study area hosts several discontinuous aquifer systems developed within fractured Precambrian rocks, Cambrian dolomitic formations, and Quaternary alluvial deposits. Groundwater occurrence is primarily controlled by secondary porosity associated with fractures, faults, and shear zones, whereas recharge largely depends on episodic rainfall and localized infiltration along wadi beds (Lachassagne et al. 2021; El Ayady et al. 2023). The drainage network is dominated by ephemeral streams, which only flow during short-lived rainfall events but may constitute locally important infiltration pathways. Owing to the scarcity of perennial rivers, groundwater is the primary source of water for domestic and agricultural uses (Scanlon et al. 2006; Taylor et al. 2013).

Climatically, the region is arid to semi-arid, with mean annual rainfall generally below 150 mm and mean annual temperatures ranging from about 20 to 25 °C. Evapotranspiration largely exceeds precipitation, which strongly limits natural recharge (El Qorchi et al. 2023). Elevation ranges from approximately 900 to 2500 m above sea level, and precipitation generally decreases from west to east under the orographic influence of the High Atlas. Vegetation cover is sparse and dominated by xerophytic shrubs, while soils are generally shallow and weakly developed.

This geological, structural, hydrogeological, and climatic setting makes the Imiter region particularly well-suited for evaluating integrated approaches to groundwater potential mapping. The strong structural control, lithological heterogeneity, and widespread hydrothermal alteration make it a relevant natural laboratory for testing the combined use of remote sensing, morphostructural analysis, and geophysical support in arid mountainous environments (Ben Sayah et al. 2023; Echogdali et al. 2022; Ikirri et al. 2023).

3 Materials and Methods

The methodological approach adopted in this study integrates multisource remote sensing, terrain analysis, morphostructural mapping, hydrothermal alteration indicators, and independent radiometric validation for groundwater potential mapping in the Imiter region, central Anti-Atlas, Morocco (Malczewski 2006; Echogdali et al. 2022; Ikirri et al. 2023; El Ayady et al. 2023). The workflow was implemented in a GIS environment and included five main steps: (i) preparation of the thematic input layers; (ii) reclassification of each factor according to its expected hydrogeological significance; (iii) weighted overlay integration to generate the groundwater potential zone (GWPZ) map; (iv) calculation of independent radiometric ratios from airborne geophysical data; and (v) point-based validation of the GWPZ map using U/Th and Th/K indicators (Maden and Akaryali 2015; Shebl et al. 2023; Gobashy et al. 2024). As shown in Fig. 3, the overall methodological workflow summarizes the sequence of data processing, integration, and validation steps applied in this study.

3.1 Data sources and thematic layers

The final groundwater potential model was based on eight thematic factors selected to represent the main structural, morphometric, surface, drainage, and hydrothermal

controls on groundwater occurrence in the Imiter region. These factors were: lineament density, topographic wetness index (TWI), slope, drainage density, normalized difference vegetation index (NDVI), carbonate alteration, kaolinite alteration, and Fe^{3+} alteration.

The SRTM digital elevation model was used to derive slope, TWI, and drainage density (Farr et al. 2007; Beven and Kirkby 1979). Sentinel-2 imagery was used to calculate NDVI as a proxy for vegetation expression and surface moisture conditions

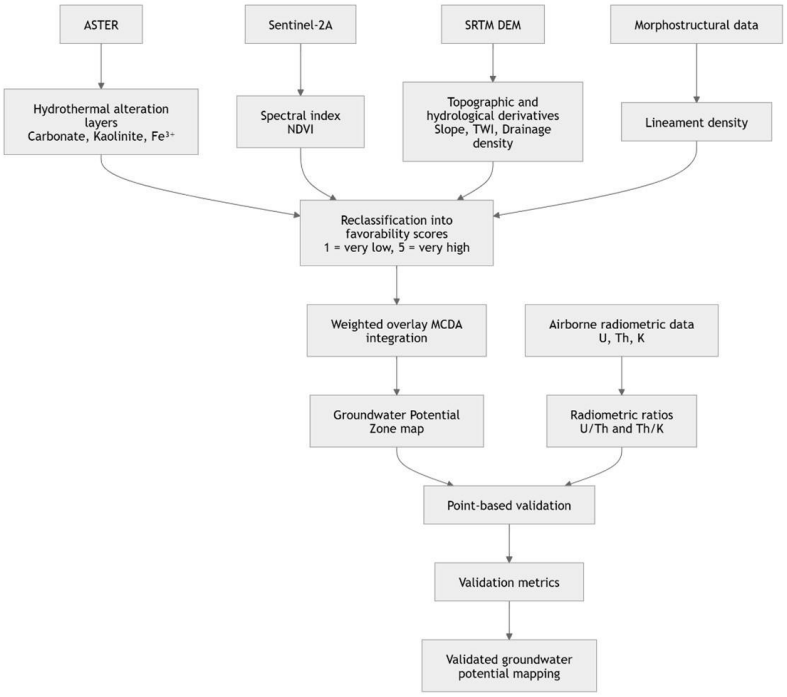


Fig. 3 Methodological workflow used for groundwater potential mapping and geophysical validation in the Imiter region.

(Drusch et al. 2012; Tucker 1979). Lineament density was derived from morphostructural interpretation and density mapping of extracted lineaments (Lachassagne et al. 2021; Kamaraj et al. 2023; Benjmel et al. 2022).

Hydrothermal alteration layers, namely carbonate, kaolinite, and Fe^{3+} alteration, were derived from ASTER VNIR–SWIR data and previous alteration mapping in the Imiter area (Abrams and Yamaguchi 2019; Ben Sayah et al. 2023). Airborne radiometric data, represented by uranium (U), thorium (Th), and potassium (K), were used only for independent validation and were not included among the predictive factors of the weighted overlay model (Maden and Akaryali 2015; Shebl et al. 2023; Gobashy et al. 2024; Hami et al. 2026).

The lithological setting of the Imiter inlier served as the geological background for interpretation, but lithology was not integrated as a weighted factor in the final model. Similarly, elevation was considered part of the regional physiographic context but was not retained as an independent predictive layer in the final weighted overlay (Subramani et al. 2024; Ayadi et al. 2025).

3.2 ASTER-derived hydrothermal alteration layers

ASTER VNIR–SWIR data were used to incorporate hydrothermal alteration information into the groundwater potential model (Abrams and Yamaguchi 2019; Ben Sayah et al. 2023). The alteration layers used in the present study were extracted from the previously published mineralogical mapping of the Imiter region, where ASTER imagery was processed using geometric correction, ortho-rectification, principal component analysis, band ratios, and thematic classification (Ben Sayah et al. 2023). The alteration indicators retained here were carbonate alteration, kaolinite alteration, and Fe^{3+} alteration.

These three alteration layers were not interpreted as direct evidence of groundwater occurrence. Instead, they were considered indirect indicators of past fluid-rock interaction, mineralogical transformation, and structurally weakened domains (Shebl et al. 2023; Gobashy et al. 2024). In a fractured hard-rock environment such as Imiter, hydrothermal alteration may coincide with zones where permeability has been enhanced by tectonic deformation, fracturing, and fluid circulation (Lachassagne et al. 2021; Ben Sayah et al. 2023; Hami et al. 2026). Therefore, the separate integration of carbonate, kaolinite, and Fe^{3+} alteration layers was preferred over a single composite alteration factor to preserve the distinct spatial contribution of each alteration indicator.

As shown in Figs. 4–5–6, the ASTER-derived hydrothermal alteration layers display distinct but complementary spatial patterns across the Imiter region. Carbonate alteration is primarily expressed as localized anomalies, particularly in the northern to northwestern sectors, suggesting zones influenced by hydrothermal fluid circulation and possible structurally controlled alteration. Kaolinite alteration appears more diffuse and spatially extended, especially toward the northern and northeastern parts of the study area, where it may reflect clay-rich hydrothermal transformation and weakened rock domains. In contrast, Fe^{3+} alteration shows a more heterogeneous distribution, with anomalies mainly associated with oxidized or near-surface alteration zones. These spatial differences justify the separate integration of the three alteration

layers in the groundwater potential model, as they represent complementary indicators of fluid–rock interaction, mineralogical transformation, and structurally modified domains.

As summarized in Table 1, the main ASTER band ratios used to identify hydrothermal alteration indicators highlight the spectral responses associated with ferric oxides, ferrous silicates, carbonate-bearing minerals, and clay minerals such as kaolinite.

Table 1 ASTER band ratios used for hydrothermal alteration mapping in the Imiter region.

Hydrothermal indicator	**ASTER band ratio**
Ferric oxides	3/4
Fe^{3+}	2/1
Ferrous silicates	5/4
Carbonate / chlorite / epidote	(7 + 9) / 8
Kaolinite	7/5

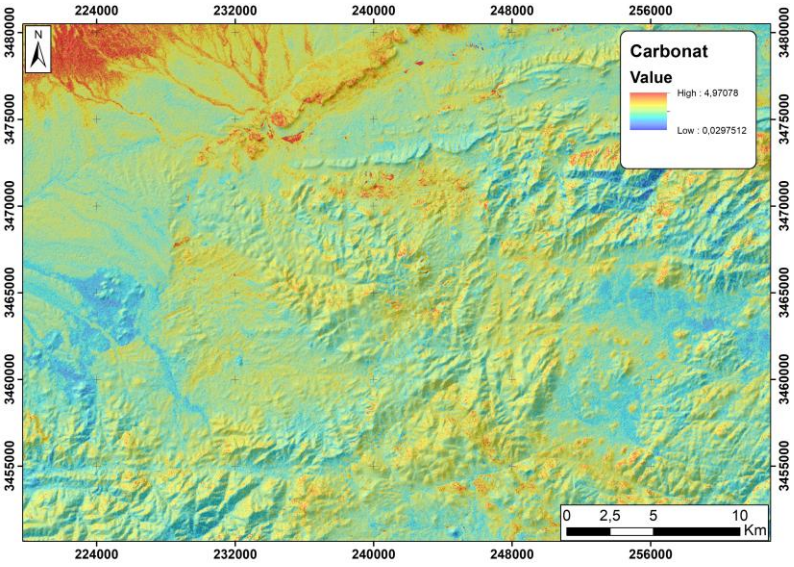


Fig. 4 ASTER-derived hydrothermal alteration layer: carbonate alteration

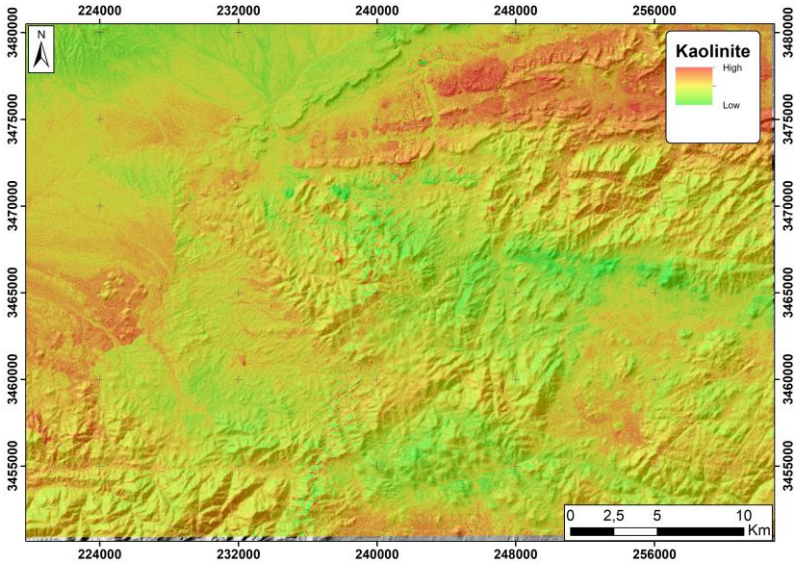


Fig. 5 ASTER-derived hydrothermal alteration layer: kaolinite alteration.

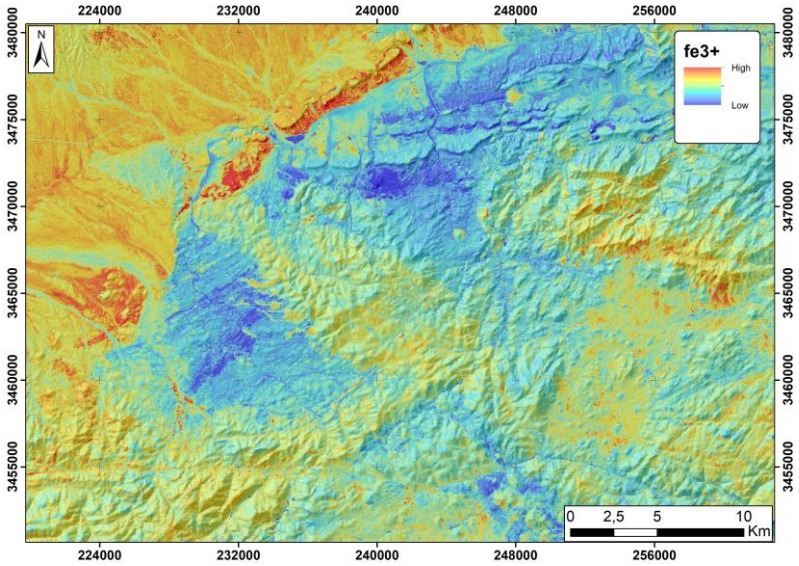


Fig. 6 ASTER-derived hydrothermal alteration layer: Fe^{3+} alteration.

3.3 Terrain-derived morphometric factors

Terrain-derived factors were extracted from the SRTM digital elevation model because topography strongly controls runoff, infiltration, surface-water concentration, and local recharge conditions in arid mountainous environments (Farr et al. 2007; Beven and Kirkby 1979).

Slope was used to represent the influence of terrain steepness on infiltration and runoff. Gentle slopes were considered more favorable to groundwater occurrence because they

promote water retention and infiltration, whereas steep slopes were considered less favorable because they favor rapid runoff and reduce percolation time. As shown in Fig. 7, low-slope areas are widely distributed across the western and central parts of the study area, indicating zones where infiltration and surface-water retention are more likely to occur. In contrast, steeper slopes are mainly concentrated in the southern, southeastern, and, locally, northeastern mountainous sectors, where runoff processes are expected to dominate infiltration. This spatial contrast supports using slope as a morphometric factor in the groundwater potential model, as it helps distinguish relatively favorable infiltration zones from areas with rapid surface drainage.

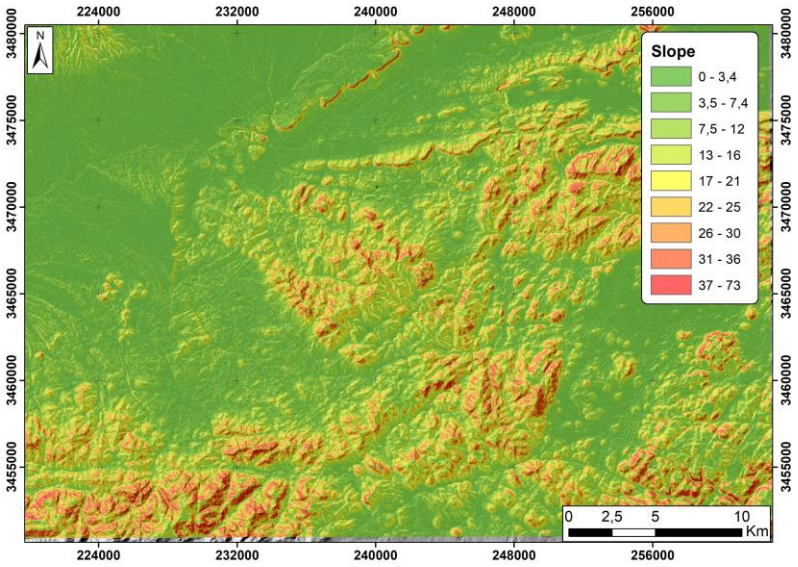


Fig. 7 Slope map derived from SRTM DEM and used in the groundwater potential model.

The topographic wetness index was used to represent the tendency of the terrain to accumulate water (Beven and Kirkby 1979). Higher TWI values were considered more favorable because they indicate zones with greater potential for surface moisture persistence and localized infiltration. As shown in Fig. 8, higher TWI values are mainly concentrated along valley bottoms, drainage corridors, and low-gradient concave areas, where surface runoff is more likely to converge and remain available for infiltration. In contrast, lower TWI values generally characterize ridges and steeper slopes, where rapid runoff limits water retention. This spatial organization supports using TWI as a hydrological terrain factor in the groundwater potential model by identifying sectors where topographic conditions favor moisture accumulation and potential recharge.

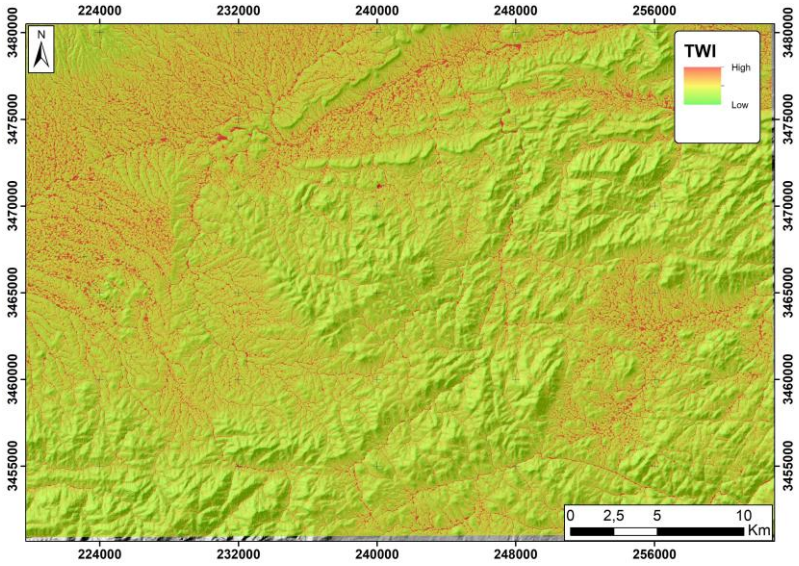


Fig. 8 Topographic wetness index (TWI) map used as an indicator of potential moisture accumulation.

Drainage density was derived from the extracted drainage network and used as an indicator of runoff organization and potential concentration of surface flow. In this study, higher drainage density values were considered more favorable because they may indicate better-developed drainage corridors where localized infiltration can occur, particularly along ephemeral stream channels and structurally controlled wadis (Echogdali et al. 2022; El Ayady et al. 2023). As shown in Fig. 9, the drainage density map reveals a heterogeneous drainage organization, with relatively high values mainly concentrated along incised valleys and structurally guided flow paths. These sectors may enhance episodic recharge during rainfall events by concentrating surface runoff and promoting localized infiltration along permeable or fractured zones. Conversely, low drainage-density areas may reflect poorly developed surface-flow networks or sectors where runoff concentration is limited. This spatial pattern supports the integration of drainage density as a complementary hydrological factor in the groundwater potential model, while recognizing that its influence depends on its coincidence with favorable slope, TWI, and structural conditions.

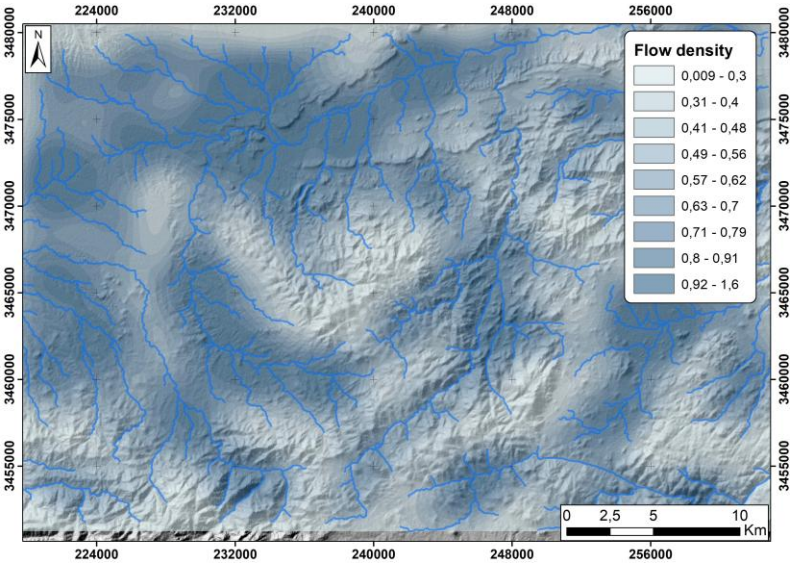


Fig. 9 Drainage density map derived from the drainage network of the Imiter region.

3.4 Lineament density

Lineament density was included as a key structural factor because groundwater occurrence in the Imiter region is strongly controlled by fracture-related secondary permeability (Lachassagne et al. 2021; El Ayady et al. 2023). Lineaments were extracted from morphostructural interpretation supported by terrain analysis, hillshade visualization, and directional filtering. The extracted lineaments were checked against the known structural framework of the Anti-Atlas in order to retain geologically meaningful fracture trends (Atif et al. 2022; Ben Sayah et al. 2023).

The lineament density map (Fig. 10) highlights a dense network of structural discontinuities, particularly in the central and eastern parts of the study area, where fracture concentration is more pronounced. These zones are interpreted as structurally favorable domains because high lineament density may enhance secondary permeability, hydraulic connectivity, and preferential groundwater circulation. Conversely, areas with lower lineament density are considered less favorable because they indicate weaker structural connectivity and reduced potential for subsurface flow. This spatial distribution justifies assigning lineament density the strongest relative influence in the weighted overlay model.

3.5 Sentinel-2 NDVI

Sentinel-2 imagery was used to calculate the normalized difference vegetation index (NDVI), which was included as a secondary indicator of surface conditions (Drusch et al.

2012; Tucker 1979). NDVI was calculated using the near-infrared and red bands according to:

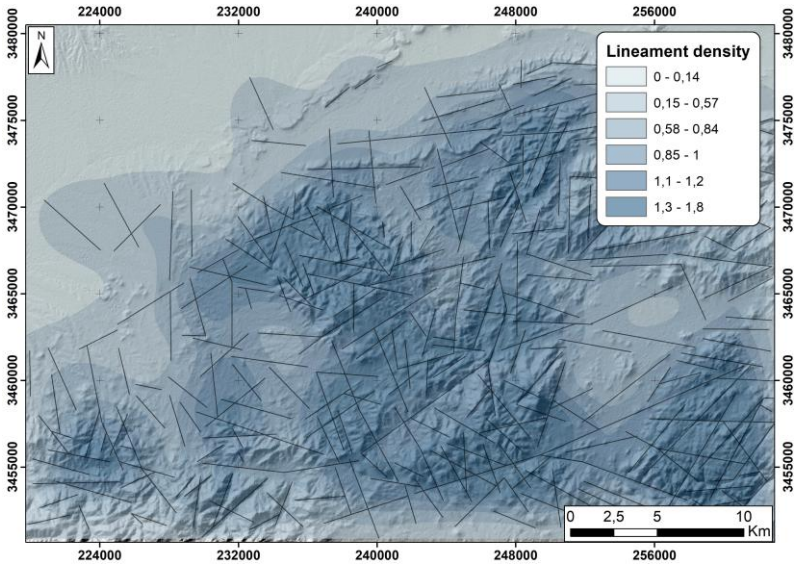


Fig. 10 Lineament density map used as a structural indicator of secondary permeability.

$$NDVI = \frac{NIR - Red}{NIR + Red} \tag{1}$$

where NIR corresponds to Sentinel-2 Band 8, and Red corresponds to Band 4.

In the arid Imiter region, vegetation cover is generally sparse; therefore, NDVI was not interpreted as a dominant groundwater indicator. Instead, it was used as a complementary proxy for relatively favorable surface moisture conditions and localized vegetation response (Tucker 1979; El Ayady et al. 2023). As shown in Fig. 11, the NDVI map indicates generally low vegetation activity across most of the study area, consistent with the arid climatic context. However, localized higher NDVI values occur mainly along valley bottoms, drainage corridors, and low-lying sectors where moisture availability may be relatively higher. These areas may reflect zones of localized water retention, episodic recharge, or vegetation response controlled by near-surface moisture. Accordingly, NDVI was integrated as a complementary surface indicator in the groundwater potential model, with lower influence than structural and morphometric factors.

3.6 Reclassification of thematic layers

All thematic layers were harmonized within the same GIS environment prior to model integration. They were resampled, clipped to the study area, and reclassified into ordinal favorability scores. The reclassification scheme was designed to translate each spatial variable into a common suitability scale ranging from 1 to 5, where 1 represents the lowest groundwater favorability and 5 the highest (Malczewski 2006; Echogdali et al. 2022; Ikirri et al. 2023). As summarized in Table 2, the reclassification thresholds reflect the relative contribution of each thematic factor to groundwater favorability based on their hydrogeological significance.

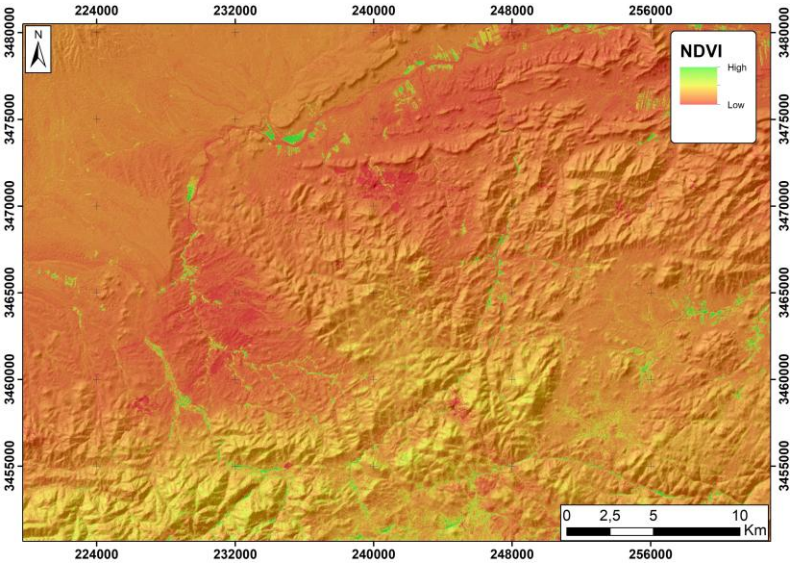


Fig. 11 Normalized difference vegetation index (NDVI) map derived from Sentinel-2 imagery.

Table 2 Reclassification scheme of thematic factors used in the weighted overlay model.

Factor	Class 1	Class 2	Class 3	Class 4	Class 5
Slope (°)	> 30	20–30	10–20	5–10	0–5
NDVI	−0.33–−0.11	−0.11–0.10	0.10–0.32	0.32–0.53	0.53–0.75
TWI	1.49–6.13	6.13–10.77	10.77–15.41	15.41–20.04	20.04–24.68
Drainage density	0.01–0.32	0.32–0.63	0.63–0.94	0.94–1.25	1.25–1.56
Lineament density	0.00–0.35	0.35–0.70	0.70–1.05	1.05–1.40	1.40–1.75
Carbonate alteration	0.03–1.94	1.94–1.98	1.98–2.02	2.02–2.06	2.06–4.97

Kaolinite alteration	−0.32–0.82	0.82–0.84	0.84–0.86	0.86–0.87	0.87–1.03
Fe^{3+} alteration	0.42–0.93	0.93–0.97	0.97–1.00	1.00–1.05	1.05–4.68

3.7 Weighted overlay integration

The groundwater potential map was generated using a weighted overlay MCDA approach. Each reclassified thematic layer was multiplied by its relative influence and then summed to obtain a groundwater potential index (Malczewski 2006; Echogdali et al. 2022; Kamaraj et al. 2023). The model can be expressed as:

$$GWPZ = \sum_{i=1}^{n} W_i \times X_i \quad (2)$$

where GWPZ is the groundwater potential index, W_i is the relative influence weight assigned to factor i, X_i is the reclassified favorability score of factor i, and n is the number of thematic factors. The final model included eight factors. The relative influence values were assigned based on the hydrogeological importance of each factor in the fractured, arid context of the Imiter region. Lineament density was assigned the strongest influence because it represents fracture-related secondary permeability, which is considered the dominant control on groundwater circulation (Lachassagne et al. 2021; El Ayady et al. 2023). TWI, slope, and drainage density were given intermediate weights because they control infiltration, runoff redistribution, and moisture accumulation (Beven and Kirkby 1979; Farr et al. 2007). The ASTER-derived alteration layers were included as process-based indicators of fluid-rock interaction and structurally modified domains (Abrams and Yamaguchi 2019; Ben Sayah et al. 2023; Shebl et al. 2023). NDVI was assigned a lower weight because vegetation cover is sparse in the study area and therefore acts only as a complementary surface proxy (Tucker 1979; Drusch et al. 2012).

As presented in Table 3, the relative influence values reflect the dominant role of structural and terrain-related factors in controlling groundwater favorability in the study area.

Table 3 Relative influence weights used in the weighted overlay model.

Thematic factor	Relative influence (%)	Rank

Lineament density	24	1
TWI	16	2
Slope	14	3
Drainage density	13	4
Carbonate alteration	10	5
Kaolinite alteration	9	6
NDVI	8	7
Fe^{3+} alteration	6	8
Total	100	–

After weighted overlay integration, the resulting groundwater potential index was reclassified into five ordinal groundwater potential classes: very low, low, moderate, high, and very high. These classes were used for regional interpretation and for subsequent comparison with independent geophysical validation indicators.

3.8 Geophysical validation using U/Th and Th/K ratios

Independent geophysical validation was performed using airborne radiometric data. Single-band uranium (U), thorium (Th), and potassium (K) layers were used to calculate two radiometric ratios: U/Th and Th/K. These ratios were not included in the weighted overlay model and were used only as independent indicators for validation (Maden and Akaryali 2015; Shebl et al. 2023; Gobashy et al. 2024).

The U/Th ratio was used as a relative indicator of uranium enrichment relative to thorium and was interpreted as a possible marker of fluid circulation and radiometric contrast within structurally influenced domains. The Th/K ratio was used as an additional radiometric indicator related to lithological and alteration contrasts. Because the radiometric layers were standardized before ratio calculation, the resulting ratios

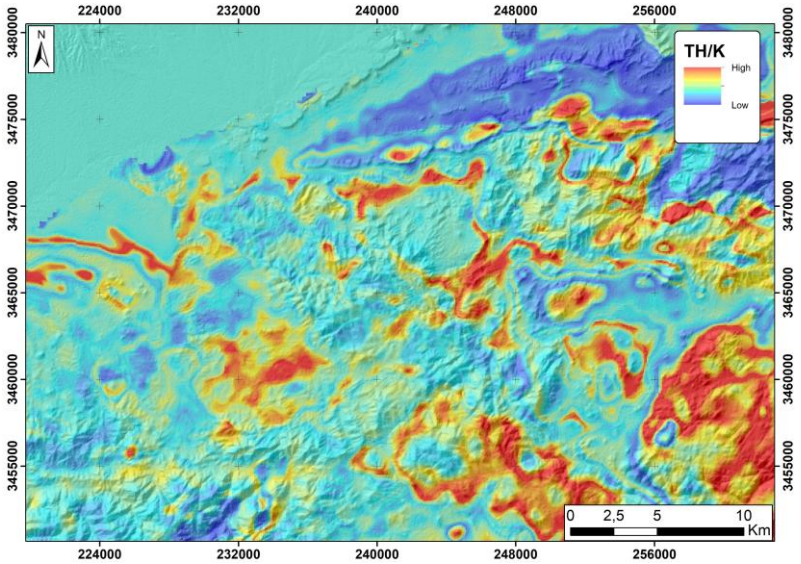


Fig. 12 Radiometric validation map derived from airborne geophysical data: Th/K ratio.

were interpreted as relative spatial indicators of anomaly contrast rather than as absolute geochemical values (Maden and Akaryali 2015; Thiam et al. 2023; Gobashy et al. 2024).

The radiometric ratios were calculated as follows:

$$U/Th = \frac{U}{Th} \tag{3}$$

$$Th/K = \frac{Th}{K} \tag{4}$$

As shown in Fig. 12–13, the Th/K and U/Th ratio maps reveal spatially heterogeneous radiometric anomalies across the Imiter region. The Th/K ratio shows the clearest spatial correspondence with the predicted groundwater-favorable zones, particularly along structurally organized and hydrothermally influenced domains. This agreement suggests that Th/K captures lithological and alteration-related contrasts that are consistent with the spatial organization of the GWPZ model. The U/Th ratio provides complementary information by highlighting radiometric contrasts that may be associated with fluid circulation and structurally controlled pathways. Although neither ratio provides direct evidence of groundwater occurrence, their spatial agreement with high- and moderate-potential zones supports the model's physical plausibility. It reinforces its use as a regional groundwater prospectivity tool.

3.9 Point-based validation procedure

A point-based validation was carried out to quantify the spatial agreement between the predicted GWPZ classes and the independent radiometric indicators. A total of 5307 validation points were used. For each point, values from the final GWPZ map

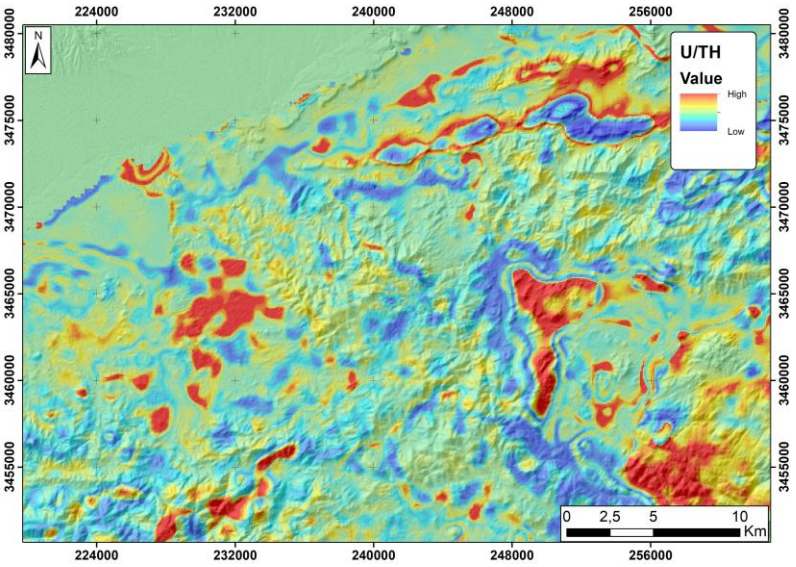


Fig. 13 Radiometric validation map derived from airborne geophysical data: U/Th ratio.

and from the U/Th and Th/K ratio maps were extracted using the "Extract Multi Values to Points" tool in ArcGIS.

The extracted values were then converted into favorable and unfavorable classes to compare predicted groundwater favorability with independent radiometric responses. The validation was performed separately for U/Th and Th/K. The agreement between GWPZ classes and each radiometric ratio was evaluated using standard binary classification metrics, including accuracy, precision, recall, and F1-score (Congalton 1991; Sokolova and Lapalme 2009). The metrics were calculated as follows:

$$Accuracy = \frac{TP + TN}{TP + TN + FP + FN} \tag{5}$$

$$Precision = \frac{TP}{TP + FP} \tag{6}$$

$$Recall = \frac{TP}{TP + FN} \tag{7}$$

$$F1 = \frac{2 \times (Precision \times Recall)}{Precision + Recall} \quad (8)$$

where TP represents true positives, TN true negatives, FP false positives, and FN false negatives.

This validation procedure was designed to assess the spatial consistency of the GWPZ map with independent geophysical indicators. It should therefore be understood as a regional consistency-based validation rather than as a direct confirmation of groundwater occurrence or aquifer productivity at the well scale. Nevertheless, the observed spatial agreement between the GWPZ classes and radiometric indicators provides robust evidence of the model's reliability in capturing structurally controlled groundwater-favorability patterns.

4 Results and Discussion

4.1 Groundwater potential zonation

As shown in Fig. 14, the final groundwater potential zone (GWPZ) map displays a marked spatial contrast between favorable and unfavorable sectors across the Imiter region. Favorable zones occur as discontinuous and locally elongated patches, mainly concentrated in the central to south-central parts of the study area, with secondary favorable sectors toward the eastern and southeastern domains. This distribution is consistent with the spatial pattern of the lineament density map, which highlights structurally more connected domains in parts of the central and eastern study area. Accordingly, the favorable GWPZ sectors are interpreted as areas where fracture-related secondary permeability is likely to be enhanced and where suitable terrain conditions, organized drainage pathways, and hydrothermal alteration indicators locally support this structural control. In contrast, unfavorable sectors correspond mainly to areas where structural connectivity appears weaker and/or where morphometric conditions are less favorable for infiltration. Overall, the final GWPZ pattern suggests that groundwater favorability in the Imiter hard-rock environment is spatially heterogeneous and controlled by the combined influence of lineament density, terrain-driven water redistribution, drainage organization, and alteration-related evidence rather than by a single conditioning factor.

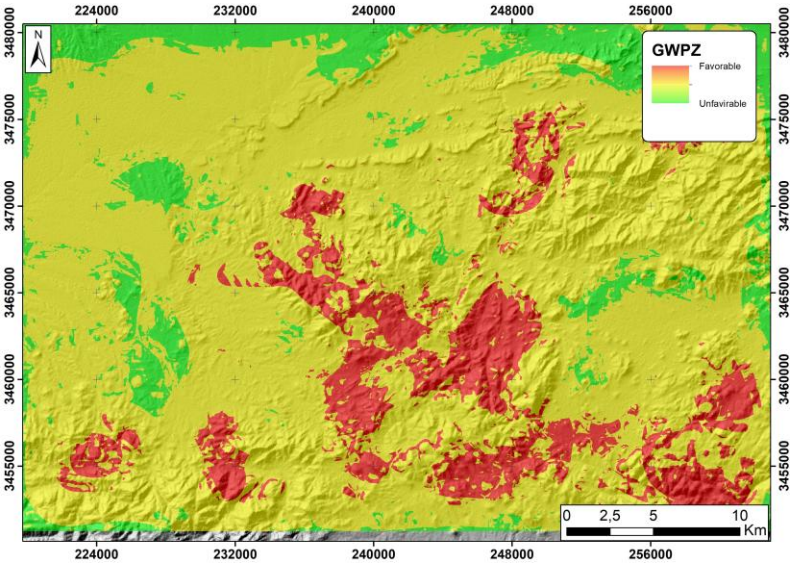


Fig. 14 Final groundwater potential zone (GWPZ) map derived from weighted overlay MCDA integration.

The distribution of the GWPZ classes highlights the dominant role of fracture-related secondary permeability in controlling groundwater favorability in the Imiter hard-rock environment (Lachassagne et al. 2021; El Ayady et al. 2023; Benjmel et al. 2022; Hilal et al. 2024). Areas with higher lineament density are interpreted as structurally more favorable because they indicate enhanced fracturing and greater hydraulic connectivity. These structural controls are reinforced locally by favorable terrain conditions, especially where TWI values indicate a higher potential for moisture accumulation and where slope conditions are conducive to infiltration rather than rapid runoff (Beven and Kirkby 1979; Echogdali et al. 2022; Slimani et al. 2024).

The contribution of ASTER-derived alteration layers further supports the interpretation of groundwater favorability as a product of coupled structural and hydrothermal processes. Carbonate, kaolinite, and Fe^{3+} alteration zones do not directly indicate groundwater occurrence, but they may mark domains affected by fluid-rock interaction and structural weakening (Ben Sayah et al. 2023; Shebl et al. 2023; Gobashy et al. 2024). Their spatial association with high-potential zones suggests that the most favorable sectors are those where fracturing, alteration, and terrain conditions converge (Hami et al. 2026; Kamaraj et al. 2023).

Overall, the final GWPZ map should be interpreted as a regional groundwater prospectivity product rather than as a direct estimate of aquifer productivity. Its main value lies in identifying priority sectors for subsequent hydrogeological and geophysical

investigations, particularly in a data-scarce arid context where direct groundwater observations are limited (Seqqam et al. 2025; Ayadi et al. 2025).

4.2 Influence of thematic factors

The spatial distribution of the groundwater potential zones reflects the combined influence of structural, topographic, drainage-related, surface, and hydrothermal alteration factors. Among the eight thematic layers integrated into the weighted overlay model, lineament density received the highest relative influence, followed by TWI, slope, drainage density, carbonate alteration, kaolinite alteration, NDVI, and Fe^{3+} alteration. This hierarchy is consistent with the hydrogeological functioning of the Imiter region, where groundwater occurrence is mainly controlled by fracture-related secondary permeability and by terrain conditions that regulate infiltration and runoff redistribution (Lachassagne et al. 2021; Kamaraj et al. 2023; Benjmel et al. 2022; Hilal et al. 2024).

Lineament density was the most influential factor in the model, with a relative influence of 24%. This weighting reflects the dominant role of fractures, faults, and structural discontinuities in hard-rock aquifer systems. In the Imiter region, areas with high lineament density are interpreted as structurally more favorable because they may correspond to zones of enhanced permeability, improved hydraulic connectivity, and preferential groundwater circulation. The spatial coincidence between high GWPZ classes and zones of dense lineament concentration therefore supports the interpretation of a structurally controlled groundwater system (Slimani et al. 2024; Ayadi et al. 2025).

The topographic wetness index represented the second most important factor, with a relative influence of 16%. TWI was included to account for the tendency of the terrain to accumulate surface moisture (Beven and Kirkby 1979). High TWI values indicate areas where water convergence and moisture persistence are more likely to occur, particularly in low-gradient or concave sectors. In the final GWPZ map, favorable groundwater zones commonly coincide with areas where high TWI values overlap with dense structural networks, suggesting that groundwater favorability increases where structural permeability and topographic accumulation potential act together (Echogdali et al. 2022; Ikirri et al. 2023).

Slope was assigned a relative influence of 14%, reflecting its direct control on the runoff–infiltration balance. Gentle slopes favor water retention and infiltration, whereas

steep slopes promote rapid surface runoff and reduce the residence time of water at the surface. In the Imiter context, low- to moderate-slope areas are therefore more favorable for groundwater recharge, especially when they occur near fractured corridors or altered zones. The slope factor primarily acts as a geomorphological modifier, enhancing or limiting the hydrogeological expression of structural controls (Subramani et al. 2024).

Drainage density contributed 13% to the final model. It was used as an indicator of the organization of surface flow and the potential concentration of runoff along drainage corridors. In arid environments, ephemeral drainage lines may play an important role in localized infiltration during short rainfall events (Scanlon et al. 2006; Taylor et al. 2013). Consequently, zones with relatively developed drainage density were considered more favorable, where they coincide with permeable structural domains. However, drainage density must be interpreted with caution, as very high drainage development may also indicate runoff-dominated conditions in certain settings (Hilal et al. 2024).

The three ASTER-derived hydrothermal alteration layers provided complementary information on fluid-rock interaction and mineralogical transformation. Carbonate alteration received a relative influence of 10%, kaolinite alteration 9%, and Fe^{3+} alteration 6%. These layers were not treated as direct indicators of groundwater presence, but as process-based proxies for zones affected by hydrothermal circulation, alteration, and structural weakening (Ben Sayah et al. 2023; Shebl et al. 2023). Carbonate and kaolinite alteration were given slightly stronger influence than Fe^{3+} because they are more closely associated with mineralogical transformation zones that may locally coincide with fractured and permeable domains. Fe^{3+} alteration was retained as a complementary indicator of oxidation and alteration contrast, but with a lower influence to avoid overemphasizing superficial radiometric or spectral effects (Gobashy et al. 2024; Hami et al. 2026).

NDVI was assigned a lower relative influence of 8%, which is appropriate for an arid region where vegetation cover is sparse and discontinuous. In this context, NDVI does not represent a primary hydrogeological control, but it may provide a secondary indication of localized surface moisture, vegetation response, or favorable near-surface conditions (Tucker 1979; Drusch et al. 2012). Its contribution to the final model is therefore complementary, helping refine the spatial expression of favorable areas without dominating the structural and terrain-derived factors (Ayadi et al. 2025).

Overall, the final GWPZ pattern is primarily controlled by the convergence of high lineament density, favorable wetness conditions, gentle-to-moderate slopes, organized drainage corridors, and hydrothermally altered domains. The model therefore emphasizes the combined role of structural permeability, morphometric suitability, and alteration-related evidence in defining groundwater-favorable zones across the Imiter region. This interpretation is consistent with the expected behavior of fractured hard-rock aquifers, where groundwater occurrence is spatially discontinuous and preferentially localized along structurally and geomorphologically favorable corridors (Lachassagne et al. 2021; Kamaraj et al. 2023; Seqqam et al. 2025).

4.3 Geophysical validation using U/Th and Th/K ratios

The final GWPZ map was evaluated using independent airborne radiometric indicators derived from uranium, thorium, and potassium data. The validation was based on the U/Th and Th/K ratios, which were calculated from single-band radiometric layers and used exclusively as external validation variables. These ratios were not included in the weighted overlay model, which avoids circularity between prediction and validation (Maden and Akaryali 2015; Thiam et al. 2023; Gobashy et al. 2024).

The U/Th ratio was used as a relative indicator of radiometric contrast potentially associated with fluid circulation and structurally influenced domains. In fractured hard-rock settings, uranium may exhibit spatial variability associated with oxidizing fluid pathways, whereas thorium is generally less mobile. Therefore, zones with relatively high U/Th values can provide indirect evidence of geochemical contrasts linked to past or present fluid circulation. In the Imiter region, several high U/Th anomalies show spatial correspondence to structurally favorable domains and to sectors classified as having moderate to high groundwater potential.

The Th/K ratio was used as a complementary radiometric indicator reflecting lithological and alteration-related contrasts. In the present validation, Th/K provided the clearest agreement with the predicted GWPZ pattern. Several zones classified as high groundwater potential coincide with marked Th/K contrasts, especially along structurally organized corridors and altered domains. This correspondence supports the interpretation that the model captures physically meaningful spatial patterns rather than only the internal logic of the weighted overlay.

The comparison between the GWPZ map and the radiometric ratios indicates that favorable groundwater zones are not randomly distributed. Instead, they tend to occur

where structural density, terrain favorability, hydrothermal alteration, and radiometric contrasts converge (Lachassagne et al. 2021; Ben Sayah et al. 2023). This spatial agreement strengthens the hydrogeological plausibility of the model, particularly in the central and south-central parts of the study area, where the final GWPZ map shows the most coherent favorable zones.

It is important to note that U/Th and Th/K are not direct indicators of groundwater presence or aquifer productivity. They are used here as independent geophysical proxies for assessing spatial consistency. The validation should therefore be interpreted as a regional-scale geophysical support for the GWPZ model, not as a substitute for site-scale hydrogeological investigation or drilling confirmation. Nevertheless, the overall consistency between the GWPZ map and the radiometric indicators strongly supports the robustness and reliability of the proposed approach in structurally controlled arid environments.

4.4 Point-based validation metrics

A point-based validation was carried out to quantitatively assess the spatial agreement between the predicted groundwater potential zones and the independent radiometric indicators. A total of 5307 validation points were used for this comparison. For each point, the corresponding values of the final GWPZ map, the U/Th ratio, and the Th/K ratio were extracted and then converted into favorable and unfavorable classes. This allowed the performance of the groundwater potential model to be evaluated separately against the two radiometric indicators (Congalton 1991; Sokolova and Lapalme 2009).

The validation results show that both radiometric ratios provide useful support for the GWPZ model, although their performance differs. The Th/K ratio yielded the strongest agreement with the predicted groundwater-favorable zones, with an accuracy of 0.601, precision of 0.632, recall of 0.857, and F1-score of 0.728. The U/Th ratio also provided acceptable validation results, with an accuracy of 0.537, a precision of 0.571, a recall of 0.828, and an F1-score of 0.676.

As summarized in Table 4, the Th/K ratio yields consistently higher performance metrics than U/Th, confirming its stronger spatial agreement with the predicted groundwater potential zones.

Table 4 Point-based validation metrics obtained from U/Th and Th/K radiometric ratios.

Radiometric indicator	Accuracy	Precision	Recall	F1-score
U/Th	0.537	0.571	0.828	0.676
Th/K	0.601	0.632	0.857	0.728

The relatively high recall values for both ratios indicate that the model successfully captures a large proportion of the zones that the radiometric indicators independently identified as favorable. This is particularly important in the context of regional groundwater exploration, where the objective is to retain potentially favorable targets for further investigation rather than to provide a definitive site-scale prediction of aquifer productivity. The higher recall obtained with Th/K suggests that this ratio is more consistent with the spatial organization of the predicted favorable GWPZ classes.

Precision values are moderate, especially for U/Th, indicating that some areas predicted as favorable by the model are not confirmed as favorable by the corresponding radiometric indicator. This behavior is expected in a regional screening model based on indirect surface and near-surface proxies. It reflects a controlled tendency toward overprediction, which is acceptable at the exploratory stage provided that the resulting favorable zones are subsequently refined using field verification and site-scale geophysical surveys.

Overall, the point-based validation confirms that the GWPZ map is not only the result of internal weighted overlay integration, but also shows measurable spatial agreement with independent airborne radiometric indicators. Among the two tested ratios, Th/K provides the most robust validation support and can therefore be considered the principal geophysical indicator for evaluating the plausibility of the final groundwater potential map. This result further supports the reliability of the proposed approach for regional-scale groundwater prospectivity assessment in structurally controlled arid environments.

4.5 Comparison with Mediterranean and North African groundwater potential studies

The results obtained in the Imiter region can be discussed within the broader context of groundwater potential mapping studies conducted in Morocco and other arid-to-semi-arid regions of North Africa. Most of these investigations have demonstrated the usefulness of remote sensing, geographic information systems, and multi-criteria

decision analysis (RS–GIS–MCDA) for delineating groundwater-favorable zones. Nevertheless, the relative influence of the conditioning factors varies considerably according to the geological setting, aquifer type, climatic conditions, spatial resolution of the input data, and validation strategy. Therefore, comparisons between groundwater potential models should not be restricted to the spatial distribution of the final classes, but should also consider the hydrogeological meaning of the selected factors, the weighting procedure, and the independence of the validation datasets.

In Morocco, several recent studies have applied GIS-based multi-criteria approaches to groundwater potential assessment in fractured and semi-arid environments. In the Tata Basin, Echogdali et al. (2022) combined remote sensing, GIS, the analytic hierarchy process, and geophysical data to delineate groundwater potential zones in a structurally controlled Anti-Atlas setting. Their approach emphasized the interaction between lithology, lineament density, slope, drainage characteristics, and other environmental variables. Similarly, Ikirri et al. (2023) mapped groundwater potential in the Ifni Basin, western Anti-Atlas, by integrating structural, lithological, morphometric, and hydrological factors within an AHP-based framework. In the Anzi sub-basin (El Ayady et al. 2023), geomatics and geophysical methods were combined to improve the identification of groundwater-favorable sectors.

These studies collectively demonstrate that groundwater occurrence in the Anti-Atlas is generally controlled by the combined effects of structural discontinuities, lithological heterogeneity, terrain morphology, and drainage organization. The present study is consistent with this regional hydrogeological interpretation, particularly regarding the dominant role of fractures and faults in enhancing secondary permeability. However, the Imiter model differs from previous Anti-Atlas investigations by explicitly integrating three ASTER-derived hydrothermal alteration indicators: carbonate alteration, kaolinite alteration, and Fe^{3+} alteration. Rather than considering hydrothermal alteration as a single composite variable or indirectly representing it through lithology, the present approach preserves the individual spatial contribution of each alteration type.

The integration of hydrothermal alteration indicators is particularly relevant in the Imiter region because the geological framework is strongly affected by tectonomagmatic and hydrothermal processes. These alteration zones are not interpreted as direct indicators of groundwater occurrence. Instead, they are considered indirect markers of fluid–rock interaction, mineralogical transformation, structural weakening, and potentially enhanced fracture permeability. Their

contribution is therefore evaluated in conjunction with lineament density, topographic wetness, slope, and drainage organization rather than independently.

Other Moroccan investigations further demonstrate that the selection of conditioning factors must be adapted to the local aquifer system. In the Kerdous inlier, Benjmel et al. (2022) integrated geological, topographic, hydrological, climatic, and structural parameters and supported the resulting groundwater potential assessment using well information and apparent resistivity data. In the Moulouya Basin, Hilal et al. (2024) applied a remote sensing, GIS, and AHP approach to evaluate the resulting groundwater potential map using borehole data. These studies benefited from direct or semi-direct hydrogeological validation datasets, whereas the Imiter region is characterized by limited availability of spatially representative borehole yield and groundwater-level data.

In the Khouribga region, Seqqam et al. (2025) integrated rainfall, lithology, slope, lineament density, drainage density, land use/land cover, distance to rivers, and potential evapotranspiration using AHP and weighted linear combination. This broader set of climatic and surface variables is appropriate for a sedimentary basin where recharge conditions, aquifer continuity, and climatic gradients exert a substantial influence on groundwater occurrence. In contrast, the Imiter study area is dominated by discontinuous hard-rock aquifers, where groundwater storage and circulation depend predominantly on secondary permeability associated with fractures, faults, shear zones, and altered domains. This difference in aquifer configuration explains why structural and morphometric factors received greater influence in the present model.

A comparable methodological contrast is observed with the Tetouan–Ras Mazari region. (Skakni et al. 2026) integrated lithology, rainfall, lineament density, land use/land cover, curvature, drainage density, slope, and TWI in a Mediterranean mountain environment characterized by fractured and karstified carbonate formations. In such a context, lithology is a major groundwater-conditioning factor because carbonate units can simultaneously serve as recharge zones and productive aquifers. In the Imiter region, however, lithological units do not form laterally continuous aquifer systems, and their hydrogeological behavior is strongly modified by tectonic fracturing and hydrothermal alteration. Consequently, lithology was retained as an interpretative geological background but was not integrated as an independent weighted factor in the final groundwater potential model.

From a methodological perspective, the present study therefore prioritizes physically interpretable factors that directly or indirectly represent the functioning of a fractured arid hard-rock aquifer. Lineament density represents secondary permeability and structural connectivity; TWI and slope describe terrain-controlled water accumulation and runoff; drainage density reflects the organization and concentration of ephemeral surface flow; NDVI provides a complementary indicator of localized surface moisture; and the three hydrothermal alteration layers characterize structurally modified and mineralogically transformed domains. This factor selection differs from that used in models developed in sedimentary, alluvial, or karstic environments, where lithology, soil properties, rainfall, and aquifer continuity may exert a stronger influence.

4.5.1 Comparison of the dominant groundwater controlling factors

Although previous groundwater potential studies consistently identified lineament density, slope, drainage density, lithology, and land use as important groundwater-conditioning factors, the relative contribution of these variables varies considerably depending on the hydrogeological context. The comparison of recent Moroccan and North African investigations indicates that no universal hierarchy of conditioning factors exists, since groundwater occurrence is fundamentally controlled by the geological evolution and hydraulic functioning of each aquifer system.

In sedimentary basins such as Khouribga and the Moulouya Basin, lithology is a dominant variable because primary porosity and aquifer continuity largely determine groundwater storage and flow (Hilal et al. 2024; Seqqam et al. 2025). Likewise, in the karstified carbonate terrains of northern Morocco, groundwater circulation is strongly governed by lithological formations that simultaneously control recharge, dissolution processes, and groundwater storage (Skakni et al. 2026). Under these geological conditions, lithology naturally carries the greatest weight in MCDA-based groundwater models.

Conversely, groundwater circulation in the Imiter region is controlled predominantly by secondary permeability developed within Precambrian crystalline and volcano-sedimentary formations. Primary porosity is generally negligible, whereas groundwater storage depends on fracture connectivity, fault intersections, weathered horizons, and hydrothermally altered zones. Consequently, lineament density is the most influential factor in the present model because it directly reflects the structural framework that governs groundwater circulation.

This interpretation is fully consistent with previous hydrogeological investigations conducted throughout the Anti-Atlas, where groundwater resources are largely associated with tectonic discontinuities rather than with lithological porosity (Echogdali et al. 2022; Ikirri et al. 2023; Benjmel et al. 2022). However, unlike previous studies, the present work does not simply consider the structural framework alone but evaluates its interaction with terrain morphology and hydrothermal alteration.

Topographic Wetness Index (TWI) represents the second most influential variable in the Imiter model. Unlike simple elevation or curvature parameters, TWI integrates both local slope and upstream contributing area, providing a physically meaningful indicator of potential water accumulation. In arid environments characterized by short-duration but high-intensity rainfall events, areas exhibiting high TWI values are more likely to concentrate runoff and promote localized infiltration, particularly where dense fracture networks are present. The importance assigned to TWI in the present study therefore reflects the combined influence of terrain-controlled water accumulation and structural permeability.

Slope also plays a significant role in controlling groundwater recharge. Gentle to moderate slopes generally favor longer surface-water residence times, thereby increasing infiltration opportunities, whereas steep slopes promote rapid runoff and limited groundwater recharge. Similar observations have been reported in numerous groundwater potential studies across North Africa (Souissi et al. 2018; Slimani et al. 2024). Nevertheless, slope alone cannot adequately explain groundwater occurrence in fractured crystalline terrains unless considered together with structural permeability and topographic convergence.

Drainage density is another factor whose interpretation strongly depends on the geological context. High drainage density is often considered unfavorable because it may indicate impermeable formations and enhanced surface runoff. However, in the Imiter region, drainage density was interpreted differently. Temporary drainage channels frequently coincide with fractured corridors where runoff generated during episodic rainfall events becomes concentrated before infiltrating through structurally weakened zones. Consequently, drainage density was not interpreted independently but in combination with lineament density, TWI, and slope. This integrated interpretation better reflects the hydrological functioning of arid hard-rock catchments.

One of the principal methodological innovations of the present study is the incorporation of three independent ASTER-derived hydrothermal alteration indicators:

carbonate alteration, kaolinite alteration, and Fe^{3+} alteration. Previous groundwater potential investigations generally represented hydrothermal alteration indirectly through lithological mapping or did not explicitly consider alteration-related information. In contrast, the present approach preserves the individual spatial contribution of each alteration indicator.

The hydrogeological significance of these alteration layers should not be interpreted as direct evidence of groundwater occurrence. Instead, hydrothermal alteration reflects past fluid circulation, mineralogical transformation, weathering processes, and localized structural weakening that may enhance fracture permeability. Carbonate alteration commonly marks hydrothermal fluid pathways associated with fault systems; kaolinite alteration reflects advanced argillic weathering and rock transformation; whereas Fe^{3+} anomalies often indicate oxidation processes related to hydrothermal activity. Their combined occurrence, therefore, provides valuable indirect information about structurally favorable groundwater environments.

The relatively low weight assigned to NDVI is also consistent with the environmental characteristics of the study area. Vegetation cover remains sparse throughout most of the Imiter region because of the prevailing semi-arid climate. Consequently, vegetation anomalies provide only localized indications of near-surface moisture conditions and should not be considered primary predictors of groundwater. Assigning excessive importance to NDVI could introduce uncertainty by emphasizing isolated vegetation patches that are controlled by local anthropogenic or seasonal effects rather than by groundwater availability.

Overall, the comparison with previous Mediterranean and North African studies demonstrates that groundwater conditioning factors cannot be transferred directly from one region to another. Instead, their relative importance must reflect the dominant hydrogeological processes governing groundwater storage, recharge, and circulation. The weighting scheme adopted in the present study therefore represents an adaptation to the specific characteristics of fractured Precambrian aquifers within the Anti-Atlas rather than a universally applicable ranking.

4.5.2 Comparison of validation strategies

Validation remains one of the most critical aspects of groundwater potential mapping because it determines the reliability and practical applicability of the resulting models. Although most recent studies report satisfactory prediction accuracies, considerable

differences exist regarding the nature, quality, and independence of the validation datasets.

Most groundwater potential investigations conducted in Morocco and North Africa have validated their results using borehole locations, well productivity, groundwater levels, electrical resistivity surveys, or receiver operating characteristic (ROC) analysis. For example, Benjmel et al. (2022) combined groundwater observations with apparent resistivity measurements to evaluate the spatial consistency of the predicted groundwater potential zones. Similarly, (Hilal et al. 2024) validated the groundwater potential model using borehole information, whereas (Skakni et al. 2026) assessed model performance through groundwater occurrence data and ROC–AUC statistics. In Tunisia, Slimani et al. (2024) evaluated groundwater favorability using groundwater levels and well yield information, while Ayadi et al. (2025) compared the predictive performance of AHP and Geo-AI models using conventional hydrogeological datasets.

These validation approaches provide direct hydrogeological evidence and constitute the preferred strategy whenever representative groundwater observations are available. However, their application may be challenging in remote, arid, hard-rock environments, where boreholes are sparse, unevenly distributed, or concentrated around mining districts and inhabited areas. Under such circumstances, borehole datasets may not adequately represent the regional variability of geological and structural conditions.

The present study addresses this limitation through an alternative validation strategy based on independent airborne gamma-ray spectrometry. Two radiometric ratios, namely U/Th and Th/K, were selected as external validation datasets because they were not incorporated during the construction of the groundwater potential model. Consequently, the validation remains independent from the predictive variables and minimizes the possibility of circular reasoning between model development and model assessment.

A total of 5307 validation points were extracted from the airborne radiometric datasets and compared with the groundwater potential classes. The Th/K ratio exhibited the strongest spatial agreement with the predicted groundwater potential zones, yielding an overall accuracy of 0.601, precision of 0.632, recall of 0.857, and F1-score of 0.728. The U/Th ratio yielded complementary results, with an overall accuracy of 0.537, precision of 0.571, recall of 0.828, and F1-score of 0.676. These results indicate that the groundwater potential model successfully identifies most areas with favorable

radiometric signatures indicative of structural alteration and hydrothermal fluid circulation.

Unlike conventional groundwater observations, airborne radiometric ratios do not directly measure groundwater occurrence, transmissivity, or aquifer productivity. Instead, they provide indirect information on lithological variability, hydrothermal alteration, weathering intensity, and geochemical processes that may influence fracture development and subsurface permeability. Consequently, the radiometric validation performed in the present study should be interpreted as an independent assessment of spatial consistency rather than a direct hydrogeological verification.

The relatively high recall values for both radiometric indicators demonstrate that the proposed workflow successfully captures most structurally favorable zones. Meanwhile, the moderate precision values suggest that some predicted corresponding radiometric signatures do not confirm favorable areas. Such behavior is expected for regional groundwater exploration models because groundwater occurrence depends on numerous subsurface factors that cannot be fully represented by surface or airborne observations alone.

Compared with previous studies, the validation framework proposed here offers several methodological advantages. First, the validation dataset remains entirely independent from the variables used to construct the groundwater potential model. Second, the large number of validation points significantly reduces local sampling bias and improves statistical robustness at the regional scale. Third, the combined use of U/Th and Th/K ratios provides complementary information on hydrothermal alteration, weathering intensity, and structural discontinuities, which is particularly relevant in mineralized Precambrian terrains such as the Imiter district.

Nevertheless, some limitations should also be acknowledged. Airborne radiometric data represent surface or near-surface geochemical conditions and therefore cannot replace direct hydrogeological observations such as pumping tests, transmissivity measurements, groundwater levels, or borehole yields. Future investigations should integrate these conventional datasets, whenever available, to further strengthen the hydrogeological validation of the proposed groundwater potential model. Despite these limitations, the independent radiometric validation adopted in the present study constitutes a robust regional-scale assessment that complements conventional groundwater exploration techniques and provides additional confidence in the spatial reliability of the predicted groundwater potential zones.

4.5.3 Scientific contribution and transferability of the proposed workflow

The comparative analysis presented above demonstrates that groundwater potential mapping has progressively evolved from simple GIS overlay techniques towards more physically meaningful multi-source integration frameworks. While previous studies have successfully combined geological, geomorphological, hydrological, climatic, and land-use variables using AHP or other MCDA approaches, relatively few investigations have explicitly incorporated hydrothermal alteration indicators and independent geophysical datasets into both model construction and validation.

The present study contributes to this evolving framework through several methodological improvements specifically designed for fractured hard-rock aquifers. First, instead of considering hydrothermal alteration as a secondary geological descriptor, three independent ASTER-derived alteration indicators, namely carbonate, kaolinite, and Fe^{3+} alteration, were incorporated separately into the weighted overlay model. This strategy preserves the individual hydrogeological significance of each alteration type and enables a more detailed representation of structurally weakened zones that may enhance groundwater circulation.

Second, the final weighting scheme was established according to the dominant hydrogeological processes governing groundwater occurrence within the Precambrian formations of the Anti-Atlas. Unlike sedimentary or karstic environments where lithology frequently dominates groundwater storage, groundwater occurrence in the Imiter district is primarily controlled by fracture connectivity, fault intersections, weathered horizons, and hydrothermal fluid pathways. Consequently, the adopted weighting hierarchy reflects the geological functioning of fractured crystalline aquifers rather than a generalized weighting scheme derived from other geological environments.

A third contribution concerns the validation methodology. Most previous groundwater potential studies relied on groundwater observations, borehole productivity, electrical resistivity measurements, or ROC-based statistical evaluation. Although these approaches provide valuable hydrogeological evidence, they often remain constrained by the limited spatial distribution of field observations. In contrast, the present study employed two independent airborne radiometric ratios (U/Th and Th/K) exclusively for model validation. Because these variables were intentionally excluded from the predictive model, they provide an independent assessment of the spatial consistency

between predicted groundwater potential zones and regional geochemical signatures associated with structural alteration and hydrothermal processes.

The use of more than 5300 independent validation points further improves the statistical robustness of the evaluation. Rather than relying on a limited number of boreholes concentrated in accessible locations, the validation covers the entire study area, providing a regional-scale assessment of model consistency. The relatively high recall values for both radiometric indicators indicate that the proposed workflow successfully identifies most structurally favorable groundwater zones. In contrast, the corresponding precision values suggest that the model intentionally remains conservative by preserving additional exploration targets. Such behavior is generally desirable during regional groundwater exploration because false negatives may lead to the omission of potentially productive sectors.

Beyond its application to the Imiter district, the proposed workflow offers a reproducible framework for groundwater exploration in structurally controlled hard-rock environments. The integration of remote sensing, GIS, hydrothermal alteration mapping, morphometric analysis, and independent geophysical validation may be adapted to other Precambrian basement terrains throughout the Anti-Atlas and comparable arid regions where conventional hydrogeological information remains scarce. Nevertheless, the weighting coefficients adopted in the present study should not be transferred directly to other regions without local calibration. Their relative importance depends on geological structure, climatic conditions, geomorphology, weathering intensity, aquifer type, and the availability of independent validation datasets.

Finally, the present study highlights the importance of combining physically interpretable conditioning factors with independent validation strategies rather than relying solely on statistical prediction accuracy. Although advanced machine-learning algorithms have recently demonstrated promising predictive capabilities, physically based MCDA approaches remain particularly attractive in data-scarce environments because each conditioning factor can be directly interpreted in terms of groundwater processes. This transparency facilitates hydrogeological interpretation, improves reproducibility, and supports practical decision-making for groundwater exploration and sustainable water-resource management in arid hard-rock regions.

5 Conclusions

This study developed an integrated groundwater potential mapping approach for the Imiter region, in the central Anti-Atlas, Morocco, by combining multisource remote sensing, terrain-derived indices, morphostructural information, hydrothermal alteration mapping, and independent airborne radiometric validation. The final model was based on eight thematic factors: lineament density, topographic wetness index, slope, drainage density, NDVI, carbonate alteration, kaolinite alteration, and Fe^{3+} alteration. These factors were selected to represent the main controls on groundwater favorability in an arid fractured hard-rock environment, where groundwater occurrence is mainly governed by secondary permeability, terrain-driven infiltration, drainage organization, and fluid-rock interaction.

The resulting groundwater potential zone map highlights a clear spatial organization of favorable and unfavorable sectors across the Imiter region. High-potential zones are mainly concentrated in structurally favorable domains, particularly where dense lineament networks coincide with suitable topographic wetness conditions, moderate slopes, organized drainage corridors, and hydrothermal alteration signatures. This spatial pattern confirms that groundwater favorability in the study area is not randomly distributed, but preferentially controlled by the convergence of fracture-related permeability, morphometric conditions, and alteration-related evidence.

Independent geophysical validation using U/Th and Th/K radiometric ratios provided additional support for the model's physical plausibility. The point-based validation performed on 5307 samples showed that the Th/K ratio gave the strongest agreement with the predicted groundwater-favorable zones, with an accuracy of 0.601, precision of 0.632, recall of 0.857, and F1-score of 0.728. The U/Th ratio also provided complementary validation support, with an accuracy of 0.537, precision of 0.571, recall of 0.828, and F1-score of 0.676. These results indicate that the model has a satisfactory ability to detect favorable zones at the regional scale. However, it should be interpreted as a prospectivity and prioritization tool rather than as a direct predictor of groundwater productivity.

Compared with conventional groundwater potential studies based mainly on lithology, rainfall, land use, and field water points, the present workflow emphasizes the specific hydrogeological context of the Imiter region. The separate integration of carbonate, kaolinite, and Fe^{3+} alteration layers, together with lineament density and radiometric validation, provides a more adapted framework for fractured, hydrothermally altered,

and data-scarce hard-rock terrains. This represents a useful complement to classical RS–GIS–MCDA approaches, particularly where direct hydrogeological observations remain limited.

The generated GWPZ map can support regional groundwater exploration by identifying priority sectors for future field verification and site-scale geophysical surveys. In particular, zones classified as high to very high potential should be considered as first-order targets for complementary investigations such as electrical resistivity tomography, vertical electrical sounding, and targeted hydrogeological reconnaissance. Nevertheless, the map should not be used alone for drilling decisions. Its interpretation must be supported by field observations, subsurface geophysical measurements, and, ultimately, borehole confirmation.

Overall, this study demonstrates that integrating remote sensing, morphostructural analysis, hydrothermal alteration mapping, weighted overlay modelling, and independent radiometric validation provides a coherent and reproducible framework for groundwater prospectivity assessment in structurally complex arid regions. The approach developed for Imiter can be transferred to other hard-rock environments where groundwater resources are controlled by fractures, alteration zones, and spatially heterogeneous recharge conditions.

Declarations

Funding

The authors received no financial support from any organization for the submitted work. No funding was received for conducting this study or for the preparation of this manuscript.

Competing interests

The authors declare that they have no known competing financial interests or personal relationships that could have influenced the work reported in this paper.

Data availability

The datasets generated and/or analyzed during the current study are available from the corresponding author upon reasonable request.

Author contributions

El Mahdi BEN SAYAH contributed to conceptualization, writing of the original draft, review and editing. Abdelmajid RAHIMI contributed to methodology, formal analysis, investigation, and resources. Mariame KHOLAIQ contributed to supervision, scientific review, and manuscript validation. All authors read and approved the final manuscript.

References

Abrams M, Yamaguchi Y (2019) Twenty years of ASTER contributions to lithologic mapping and mineral exploration. Remote Sensing 11(11):1394 https://doi.org/10.3390/rs11111394

Atif Y, Soulaimani A, Ait Lahna A, Yaagoub D, Youbi N, Pour AB, Hashim M (2022) Structural analysis and paleostress evolution in the Imiter silver mining region, Eastern Anti-Atlas, Morocco: implications for mineral exploration. Minerals 12(12):1563 https://doi.org/10.3390/min12121563

Ayadi Y, Gentilucci M, Ncibi K, Hadji R, Hamed Y (2025) Assessment of a groundwater potential zone using geospatial artificial intelligence (Geo-AI), remote sensing (RS), and GIS tools in Majerda transboundary basin (North Africa). Water 17(3):331 https://doi.org/10.3390/w17030331

Ben Sayah EM, Rahimi A, Saber N, Kholaiq M, Maacha L (2023) Mineralogical mapping using remote sensing and geophysical data in Imiter Anti-Atlas of Morocco. Remote Sensing in Earth Systems Sciences 6:77–89 https://doi.org/10.1007/s41976-023-00082-z

Benjmel K, Amraoui F, Aydda A, Tahiri A, Yousif M, Pradhan B, Abdelrahman K, Fnais MS, Abioui M (2022) A multidisciplinary approach for groundwater potential mapping in a fractured semi-arid terrain (Kerdous Inlier, Western Anti-Atlas, Morocco). Water 14(10):1553 https://doi.org/10.3390/w14101553

Beven KJ, Kirkby MJ (1979) A physically based, variable contributing area model of basin hydrology. Hydrological Sciences Bulletin 24(1):43–69 https://doi.org/10.1080/02626667909491834

Cheilletz A, Levresse G, Gasquet D, Azizi-Samir MR, Zyadi R, Archibald DA, Farrar E (2002) The giant Imiter silver deposit: Neoproterozoic epithermal mineralization in the Anti-Atlas, Morocco. Mineralium Deposita 37:772–781 https://doi.org/10.1007/s00126-002-0317-0

Congalton RG (1991) A review of assessing the accuracy of classifications of remotely sensed data. Remote Sensing of Environment 37(1):35–46 https://doi.org/10.1016/0034-4257(91)90048-B

Drusch M, Del Bello U, Carlier S, Colin O, Fernandez V, Gascon F, Hoersch B, Isola C, Laberinti P, Martimort P, Meygret A, Spoto F, Sy O, Marchese F, Bargellini P (2012) Sentinel-2: ESA's optical high-resolution mission for GMES operational services. Remote Sensing of Environment 120:25–36 https://doi.org/10.1016/j.rse.2011.11.026

Echogdali FZ, Boutaleb S, Bendarma A, Saidi ME, Aadraoui M, Abioui M, Ouchchen M, Abdelrahman K, Fnais MS, Sajinkumar KS (2022) Application of analytical hierarchy process and geophysical method for groundwater potential mapping in the Tata Basin, Morocco. Water 14(15):2393 https://doi.org/10.3390/w14152393

El Ayady H, Mickus KL, Boutaleb S, El Morjani ZEA, Ikirri M, Echogdali FZ, Ekoa Bessa AZ, Abdelrahman K, Id-Belqas M, Essoussi S, Fnais MS, Abioui M (2023) Investigation of groundwater potential using geomatics and geophysical methods: case study of the Anzi sub-basin, Western Anti-Atlas, Morocco. Advances in Space Research 72(10):3960–3981 https://doi.org/10.1016/j.asr.2023.08.044

El Qorchi F, Yacoubi Khebiza M, Omondi OA, Karmaoui A, Pham QB, Acharki S (2023) Analyzing temporal patterns of temperature, precipitation, and drought incidents: a comprehensive study of environmental trends in the Upper Draa Basin, Morocco. Water 15(22):3906 https://doi.org/10.3390/w15223906

Farr TG, Rosen PA, Caro E, Crippen R, Duren R, Hensley S, Kobrick M, Paller M, Rodriguez E, Roth L, Seal D, Shaffer S, Shimada J, Umland J, Werner M, Oskin M, Burbank D, Alsdorf D (2007) The Shuttle Radar Topography Mission. Reviews of Geophysics 45(2):RG2004 https://doi.org/10.1029/2005RG000183

Gobashy MM, El-Sadek MA, Mekkawi MM, Araffa SAS, Ezz Eldin MM, Khalil MH (2024) Radiometric characteristics of some metallic ores and nonmetallic deposits: an example, Wadi Al-Allaqi, South Eastern Desert, Egypt. Scientific Reports 14:2443 https://doi.org/10.1038/s41598-024-52912-9

Hami A, Dairi S, Mechentel E, Abida H, Zenati N (2026) Mapping groundwater potential zones using GIS and AHP in a semi arid watershed: A case study of the Medjerda basin, northeastern Algeria. Journal of African Earth Sciences 237:106059 https://doi.org/10.1016/j.jafrearsci.2026.106059

Hilal I, Qurtobi M, Saadi R, Aqnouy M, Bouizrou I, Bouadila A, Dakak H, Abdelrahman K, Moreno-Navarro JG, Abioui M, Stitou El Messari JE, Ekoa Bessa AZ, Benmansour M (2024) Integrating remote sensing, GIS-based, and AHP techniques to delineate groundwater potential zones in the Moulouya Basin, North-East Morocco. Applied Water Science 14:122 https://doi.org/10.1007/s13201-024-02175-6

Ikirri M, Boutaleb S, Ibraheem IM, Abioui M, Echogdali FZ, Abdelrahman K, Id-Belqas M, Abu-Alam T, El Ayady H, Essoussi S, Faik F (2023) Delineation of groundwater potential area using an AHP, remote sensing, and GIS techniques in the Ifni Basin, Western Anti-Atlas, Morocco. Water 15(7):1436 https://doi.org/10.3390/w15071436

Kamaraj P, Muralitharan J, Panda B, Sabarathinam C (2023) Mapping of groundwater potential zones by integrating remote sensing, geophysics, GIS, and AHP in a hard rock terrain. Urban Climate 51:101610 https://doi.org/10.1016/j.uclim.2023.101610

Lachassagne P, Dewandel B, Wyns R (2021) Hydrogeology of weathered crystalline/hard-rock aquifers—guidelines for the operational survey and management of their groundwater resources. Hydrogeology Journal 29:2561–2594 https://doi.org/10.1007/s10040-021-02339-7

Maden N, Akaryali E (2015) Gamma ray spectrometry for recognition of hydrothermal alteration zones related to a low sulfidation epithermal gold mineralization. Journal of Applied Geophysics 122:74–85 https://doi.org/10.1016/j.jappgeo.2015.09.003

Malczewski J (2006) GIS-based multicriteria decision analysis: a survey of the literature. International Journal of Geographical Information Science 20(7):703–726 https://doi.org/10.1080/13658810600661508

Scanlon BR, Keese KE, Flint AL, Flint LE, Gaye CB, Edmunds WM, Simmers I (2006) Global synthesis of groundwater recharge in semiarid and arid regions. Hydrological Processes 20(15):3335–3370 https://doi.org/10.1002/hyp.6335

Seqqam A, Touirsi M, Najib S, Fadili A, Mehdi K, Tagma T (2025) Integrated approaches to map groundwater potential zones using AHP, GIS, and remote sensing in semi-arid

region of Morocco: case study from Khouribga area. Solid Earth Sciences 10(4):100272 https://doi.org/10.1016/j.sesci.2025.100272

Shebl A, Abdellatif M, Badawi M, Dawoud M, Fahil AS, Csamer A (2023) Towards better delineation of hydrothermal alterations via multi-sensor remote sensing and airborne geophysical data. Scientific Reports 13:7406 https://doi.org/10.1038/s41598-023-34531-y

Skakni O, Rahimi A, Hlila R, Al-Djazouli MO, Barhi H, Aoulad Mansour MR, Boukholla A (2026) Groundwater potential mapping of Tetouan–Ras Mazari (Rif Mountains, Morocco). Mediterranean Geoscience Reviews https://doi.org/10.1007/s42990-026-00235-4

Slimani FE, Zghibi A, Elomri A, Aloui S, Naeem K, Merzougui A, Msaddek MH, Chekirbene A (2024) Identification of groundwater potential recharge zones in a Tunisian anthropogenic coastal region. Journal of African Earth Sciences 209:105108 https://doi.org/10.1016/j.jafrearsci.2023.105108

Sokolova M, Lapalme G (2009) A systematic analysis of performance measures for classification tasks. Information Processing & Management 45(4):427–437 https://doi.org/10.1016/j.ipm.2009.03.002

Souissi D, Msaddek MH, Zouhri L, Chenini I, El May M, Dlala M (2018) Mapping groundwater recharge potential zones in arid region using GIS and Landsat approaches, southeast Tunisia. Hydrological Sciences Journal 63(2):251–268 https://doi.org/10.1080/02626667.2017.1414383

Soulaimani A, Ouanaimi H, Saddiqi O, Baidder L, Michard A (2018) The Anti-Atlas Pan-African belt (Morocco): overview and pending questions. Comptes Rendus Geoscience 350(6):279–288 https://doi.org/10.1016/j.crte.2018.07.002

Subramani D, Kamaraj P, Saravana Kumar U, Sabarathinam C (2024) Mapping of groundwater recharge zones in hard rock aquifer through analytic hierarchy process in geospatial platform. Water 16(11):1484 https://doi.org/10.3390/w16111484

Taylor RG, Scanlon B, Döll P, Rodell M, van Beek R, Wada Y, Longuevergne L, Leblanc M, Famiglietti JS, Edmunds WM, Konikow L, Green TR, Chen J, Taniguchi M, Bierkens MFP, MacDonald AM, Fan Y, Maxwell RM, Yechieli Y, Gurdak JJ, Allen DM, Shamsudduha M, Hiscock K, Yeh PJF, Holman I, Treidel H (2013) Groundwater and climate change. Nature Climate Change 3:322–329 https://doi.org/10.1038/nclimate1744

Thiam A, Baratoux D, Ngom PM, Jessell M, Baratoux L, Fall M, Ndiaye PM (2023) Multiparameter statistical analysis of K, Th, and U concentrations for geological mapping using airborne radiometric data. Geosciences 13(9):263 https://doi.org/10.3390/geosciences13090263

Tucker CJ (1979) Red and photographic infrared linear combinations for monitoring vegetation. Remote Sensing of Environment 8(2):127–150 https://doi.org/10.1016/0034-4257(79)90013-0

Tuduri J, Chauvet A, Ennaciri A, Barbanson L (2006) Modèle de formation du gisement d'argent d'Imiter (Anti-Atlas oriental, Maroc). Comptes Rendus Geoscience 338(4):253–261 https://doi.org/10.1016/j.crte.2005.11.010

Walsh GJ, Aleinikoff JN, Harrison RW, Burton WC, Quick JE, Benziane F, Yazidi A, Saadane A (2012) Neoproterozoic tectonic evolution of the Anti-Atlas, Morocco. Precambrian Research 216–219:23–62 https://doi.org/10.1016/j.precamres.2012.06.010